CHAPTER 32

Cingulate Subregional Neuropathology in Dementia with Lewy Bodies and Parkinson's Disease with Dementia

Brent A. Vogt, Leslie Vogt, Dushyant P. Purohit, and Patrick R. Hof

Chapter contents

The Lewy body (LB) is one of the most common markers of cingulate neuropathology; exceeded only by amyloid-β peptides. Disorders in which LBs are encountered in the cingulate gyrus include Alzheimer's disease (AD), Parkinson's disease with dementia (PDD), dementia with Lewy bodies (DLB), and aging (Saito *et al.*, 2003). Cases with LBs form 15–25% of all cases of dementia which is second only to that of pure AD (McKeith *et al.*, 1996); however, as LBs are observed in more than half of definite AD cases, they are common in AD (Ditter & Mirra, 1987). The comorbid expression of DLB and AD is still a matter of debate because key markers of both diseases are so frequently observed in the same cases (Perl *et al.*, 1998). Moreover, in addition to 'pure' forms of each of these progressive dementing diseases, their conjunction throughout the cingulate gyrus generates a complex neuropathological context in which to consider symptom etiology that still has not been resolved.

The Consensus Guidelines for DLB identified progressive mental impairment leading to dementia as the central feature of DLB (McKeith *et al.*, 1996). They also concluded that attentional impairments, visual hallucinations, and spontaneous motor features of Parkinsonism are essential diagnostic features for discriminating DLB from AD and other dementias. Although visual hallucinations may result from alterations in occipital lobe functions and progressive mental impairment results from general cortical damage, some of these symptoms do not result from primary cortical damage and little is known of how impairment of specific cingulate functions contribute to the early and progressive symptoms of DLB. A new generation of functional imaging research provides a more precise framework in which to evaluate structure/function correlates in progressive dementing disorders.

The Guidelines also suggest evaluation of a postmortem cingulate gyrus sample at 1.5 cm caudal to the anterior pole of the genu of the corpus callosum and rostral to the vertical plane at the anterior commissure (VCA). This places sampling at +3.1 cm to the VCA in Talairach coordinates (Talairach & Tournoux, 1988) and in the anterior midcingulate subregion (aMCC; Vogt *et al.*, 2003; Chapter 1). This designation for neuropathological assessment suggests that damage to aMCC should be consistent, reflected in some way via DLB symptomatology, and imaging of functional alterations should highlight involvement of this subregion. It may imply that functional and neuropathological damage at distant cingulate sites, such as in posterior cingulate and precuneal cortices (PCC, PrCC, respectively), should be more variable and less likely to participate in neuropsychological deficits and changes in glucose metabolism. Some but not all of these expectations are supported by systematic structure/function correlations throughout the cingulate gyrus.

The Parkinson's Disease Model of Neurodegeneration

The link between DLB and PD with LB deposition leads to a disease model that is a starting point for analysis of processes in cingulate cortex. The PD model emphasizes LBs in the substantia nigra and associated neurodegeneration, monoaminergic depletion and movement symptoms, and mechanisms of neurodegeneration including α-synuclein phosphorylation and nitration. Each of these views has relevance to interpreting the role of LBs in cingulate neuropathology and underpins the discourse below. However, aspects of this model have not been readily applied to cingulate neuropathology to date for a number of reasons. First, although extensive neurodegeneration is easily demonstrated in the substantia nigra, the link between LB deposition and neurodegeneration is one of speculation in cingulate cortex and LBs could actually participate in neuroprotective mechanisms (Harrower *et al.*, 2005). In addition, the presence or absence of neurodegeneration and potential mechanisms thereof are pivotal to understanding cingulate-mediated mechanisms of dementia and they may not have been clearly identified in the past because of reliance on thin paraffin sections in diagnostic procedures (i.e., thin sections decrease the resolution of laminar architecture, particularly in neurodegenerative diseases). Second, there is no doubt that dopamine (DA) is part of the PD and DLB disease process. Interestingly, however, cingulate cortex receives substantial DAergic input from the ventral tegmental area and even the substantia nigra and the greatest termination is in the rostral cingulate premotor area (rCPMA) in aMCC as discussed in detail in Chapter 7. Thus, the DAergic aspect of the PD model shrouds the fact that major monoaminergic impairments could result in cingulate-mediated movement impairment; not extrapyramidal symptoms *per se*, but certainly apraxias and dyskinesias that are relevant to organizing and guiding movement. Thus, one of the major goals of the present chapter is to evaluate cingulate neuropathology in LB diseases and to sort through expectations derived from the PD model.

Goals of this Chapter

In light of their early and prominent deposition in the cingulate gyrus in DLB, LBs provide an important focus for studying cingulate functional disruption and critical links to cingulate neurodegeneration. As aMCC is a diagnostic structure for DLB neuropathology, firm insight into the role of LBs in cingulate neuropathology is required; surprisingly, there are no systematic reviews of correlations between specific functional impairments and neuropathology in the cingulate gyrus in DLB and PDD. The subregional model of the cingulate

cortex presented in Chapter 1 serves as the basis for this first comprehensive analysis of those aspects of DLB symptoms that may be mediated by cingulate impairments. Such an analysis can be extended beyond the general counting of neurons expressing α-synuclein-expressing neurons to a laminar level of analysis so that specific linkages with neuron losses and α-synuclein and amyloid-β peptide expression can be assessed. This process is supported with precise cytoarchitectural analysis in thick sections and use of immunohistochemical standards for laminar neuron densities that are not generally available. This is a case-guided review and it provides new observations based on the four-region neurobiological model of the cingulate gyrus.

1 Evaluate the structure and topographical distribution of α-synuclein-expressing neurons (αSN) throughout cingulate cortex.

2 Link the laminar profiles of αSN to neuron losses in four cases of DLB with immunohistochemical methods.

3 Identify matches between laminar profiles of αSN, neuron loss and markers of AD pathology; amyloid-β 42 and phosphorylated tau.

4 Consider hypotheses of where DLB begins in the cingulate gyrus by providing precise laminar information on subgenual anterior cingulate cortex (sACC), aMCC, pMCC, and dorsal posterior cingulate cortex (dPCC). There is a focal point in pMCC/dPCC.

5 Briefly review the mechanisms of cingulate neurodegeneration mediated by α-synuclein phosphorylation, amyloid-β peptides, and oxidative stress and suggest how they might be linked to produce early layer V neuron losses; neurons that project heavily into subcortical motor systems.

6 Assess the functional imaging literature of DLB and PDD in the context of key symptoms, the four-region neurobiological model and findings of the present analysis.

7 Evaluate the DA hypothesis of DLB/PDD in the context of the cingulate premotor areas and visuoconstructional apraxias in terms of the pathological nidus in pMM/dPCC.

Dementia with Lewy Bodies: Symptoms and Imaging Pathological Changes

The Consensus Guidelines for the diagnosis of DLB observe disabling mental impairment progressing to dementia as a central feature, attentional impairments, and disproportionate problem solving and visuospatial difficulties that are often early (McKeith *et al.*, 1996). Any or all of these features could be attributed to damage in the cingulate cortex and, after the location and extent of cingulate neuropathology in DLB has been considered, we will explicitly consider cingulate-mediated mechanisms of impaired brain function. Additionally, fluctuating cognition, visual hallucinations, and spontaneous Parkinsonism are core features and help distinguish between DLB and AD. Studies of cerebral metabolism and atrophy are an important starting point for evaluating the role of cingulate cortex in these symptoms, although the findings to date have not been entirely consistent.

Albin *et al.* (1996) evaluated glucose metabolism in three confirmed cases of DLB; two of whom had visual hallucinations. The distribution of glucose hypometabolism on the medial surface is co-registered in Figure 32.1 to a postmortem case we used to derive the boundaries

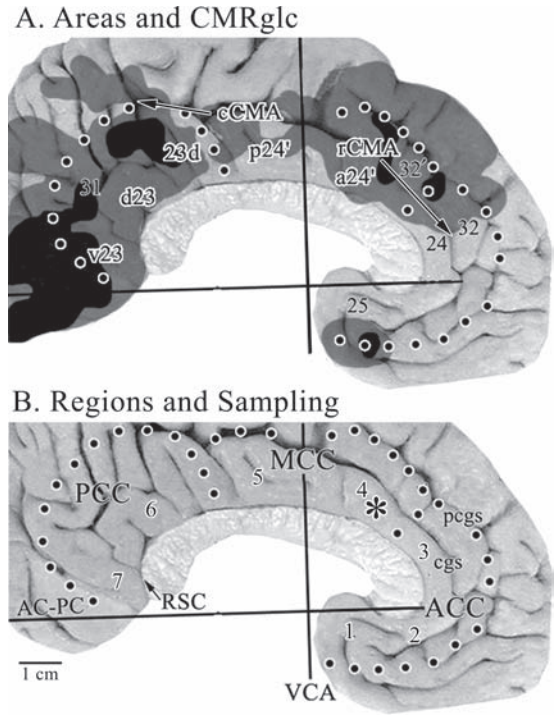

Fig. 32.1 A. Overview of cingulate organization in a control case with the major regions outlined (see B.) and the center of some areas identified. The rostral (rCMA) and caudal (cCMA) cingulate motor areas are identified along with arrows to show their approximate extent in the cingulate sulcus. Coregistered to this case is the CMRglc from the Z-score maps of Albin *et al.* (1996) for three cases with postmortem confirmed DLB. The black is for Z scores >4 and shading for scores of 3–4. B. Photograph of the medial surface of a control case used for histological comparisons with the DLB cases. The four regions are outlined with dots, retrosplenial cortex (RSC) is shown in the callosal sulcus and an asterisk identifies the sampling site for the Consensus Guidelines. Numbers 1–7 locate samples for the present assessment: 1, sACC; 2, sACC; 3, pACC; 4, aMCC; 5, pMCC; 6, dPCC; and 7, vPCC.

of each cingulate area, subregion, and region. There was almost no involvement of sACC and minor involvement of pMCC, while the greatest glucose hypometabolism was in aMCC and throughout PCC. To the extent that visual hallucinations are associated with glucose hypometabolism, it is not surprising to see the extension of the hypometabolic area from vPCC into medial visual association areas. The involvement of PCC is considered later in the context of its visuospatial and visuocontructional functions; although it is surprising that the pure DLB cases had no PCC pathological changes in spite of severe glucose hypometabolism. Although Ishii *et al*. (1998) did not reconstruct the medial surface, glucose hypometabolism occurred in most of the cerebral cortex, medial, and lateral occipital lobe differences distinguished DLB from AD, and the ACC and PCC had reductions. Finally, Burton *et al*. (2002) evaluated atrophy with voxel-based morphometry in 25 DLB cases but found no changes in the cingulate gyrus. This negative finding might reflect methodological or diagnostic problems rather than a lack of PCC involvement.

Case Tissues

This is a case-based review that considers issues of cingulate involvement in DLB that have been overlooked and support for new perspectives based on a thorough analysis of four cases with DLB. These four cases provide photographic support of the essential conclusions and are the basis for a series of hypothesis-driven observations about the impact of LB on cingulate cytology and function. The characteristics of each case are summarized in Table 32.1. Age-matched control and AD cases were also used but they are not summarized in the table. Each case received standard clinical and neuropathological evaluation with the latter including hematoxylin and eosin, silver, and thioflavin S staining of the following regions: middle and orbitofrontal gyri, rostral and caudal hippocampus, superior temporal, inferior parietal, visual and cingulate cortices, basal nucleus of Meynert, basal ganglia, amygdala, midbrain, pons, medulla, and cerebellum. The cingulate gyrus and adjacent cortex was further analyzed with 8-, 1-cm-thick blocks; one in area 9 and 7 through each cingulate subregion as shown in Figure 32.1B; two in subgenual ACC and one each in pACC, aMCC at a site equivalent to that suggested for analysis by the consensus report on DLB (asterisk in Fig. 32.1B), pMCC, dPCC/RSC, and vPCC. As each cingulate block included cortex dorsal to the cingulate gyrus, a wide range of neocortical structures were available for analysis.

TABLE 32.1 DLB/PD case characteristics

Case #/ Gender	Age at death/ Brain weight	α-Synuclein+ neurons*			Braak stage
		sACC	aMCC	dPCC	
1/F	84/1,145				Med. Temp. NFT/III
2/F	101/907				Med. Temp. NFT/III
3/M	96/1148				
		52±25	54±21	85±22	
4/F	91/756				Possible AD/V**

*Mean±SEM for #1-#3 for about 50 mm2 of layers V/VI of the gyrus; that is, for subregions not areas.

** Case #4 had extensive neuropil threads throughout the entire cingulate gyrus and few neurofibrillary tangles (NFT), while the medial temporal lobe had severe NFT; this case was not included in the counts above.

It is important to note that sections were cut 50-μm thick in a cryostat and are about 4–5 times thicker than those for hematoxylin and eosin staining. The reason for the greater thickness is that it is compatible with previous cytoarchitectural studies and localization of immunoreactive elements can be determined in this context. Studies employing paraffin sections are difficult to use to assess the exact layers and areas and this is more effectively done with thicker sections. Indeed, thinner sections make it generally more difficult to qualitatively observe changes in neuron density. The immunohistochemical protocols include preincubation steps in methanol/hydrogen peroxide and formic acid and their details have been previously published (Vogt *et al*., 2001, 2006). Only the α-synuclein (Chemicon, Temecula, CA) protocol has not been reported and it involved a reaction at a dilution of 1:5,000 following the above pretreatment, staining, and mounting as reported in the referenced articles.

The control case for neuron densities was an 80-year-old male who died of pneumonia (brain weight, 1,360 gm). In addition to a standard thionin stain, an antibody to neuron-specific nuclear binding protein (NeuN) was used to gauge neuron losses in the DLB cases because these latter cases could not be prepared with this antibody due to extended fixation. The staining of small neurons is less clear in thionin and the NeuN outlines the edges of neurons with a dark precipitate and their size, shape, and distribution are more easily identified with NeuN. A comparison of these two methods is shown for the control at high magnification in Figures 32.8 and 32.9 so these differences can be appreciated when evaluating changes in neuron density.

Structure of Cingulate Lewy Bodies

Cortical LB with a classical hyaline (eosinophic) staining is rare in cingulate cortex. Cortical LBs tends to be

granular and lack the halo found in brainstem LB where the LB is also linked to patent neurodegeneration (McKieth *et al*., 1996). A comparison of α-synuclein labeling of cingulate neurons with those in the substantia nigra shows that the former usually have a diffuse labeling without the halo structure (Sakamoto *et al*., 2002). A rare cingulate cortical LB is shown in an α-synuclein-immunoreacted section in Figure 32.2A. As this specific morphology is rare and the α-synuclein reactivity tends to be diffuse in the neuronal perikaryon, α-synuclein-positive neurons, and neurites (αSN and αSNr, respectively) are used to designate these profiles rather than LB *per se*. The subcortical LBs and αSN contain phosphorylated and non-phosphorylated neurofilaments and α-synuclein, while tau protein is not present (McKieth *et al*., 1996). Figure 32.2B shows a neuron adjacent to the one in Figure 32.2A that is immunoreactive for the AT8 antibody that was generated to tau protein with two phosphorylation sites; one at serine 202 and another at threonine 205 (Goedert *et al*., 1995). Although neurons with LBs are rare, this example provides an opportunity to demonstrate differences in each. The aggregation of neurofilaments is apparent in the tau-labeled neuron, while the αSN has a more diffuse deposit. Finally, diffuse aggregates in neurites expressing α-synuclein are also present in cingulate cortex (αSNr). In some instances these can be found in diffuse plaques as suggested in Figure 32.2D and E. The direct linkage between αSNr and plaque deposition would provide an interesting double-label study. Here we show an AT8-immunoreactive neuritic plaque in an adjacent section to suggest that the profile in the α-synulein-immunoreacted section has the correct size for a plaque in the same layer and area. As LB contain α-synuclein in DLB (Dickson, 2001) and PDD (Mattila *et al*., 2000; Braak *et al*., 2005), α-synuclein is the key marker for LB and are used to assess the present four cases in detail.

Topography of αSN, Diagnostic Sampling, and Limbic-Neocortical Transition

The Consensus Guidelines suggest a classification of DLB into three categories (brainstem predominant, limbic, and neocortical) that employ cortical samples linked to CERAD criteria (McKeith *et al*., 1996). As noted above, the cingulate sample is suggested from aMCC and it contributes to the LB score and Hishikawa *et al*. (2003) show coronal sections, including this level of cingulate cortex, in each category with a plot of ubiquitin-immunoreactive neurons. The LB score and its associated three categories assume a progression that spreads from limbic to neocortical areas along the lines of that suggested for PDD by Braak *et al*. (2003). An equally valid model for sampling would be a progressive and uniform buildup of αSN throughout the entire cingulate gyrus without regional specificity. In either instance, the aMCC sample has value as long as there is a predictable buildup in αSN in the cingulate gyrus and that in aMCC reflects this trend in some reasonable fashion.

The cingulate gyrus is comprised of a full range of cortical structures. The least differentiated extend from area 25 in sACC to caudal ectocallosal areas 33 and 26 and retrosplenial areas 29 and 30. Differentiation progresses in a dorsal and caudal fashion to include areas 24 and various parts of area 32 rostrally and neocortical areas 23 and 31 in the posterior cingulate gyrus. Areas 25/33/26 are limbic in the sense they are involved in emotion and have an undifferentiated structure, while areas 23 and 31 have a well-differentiated layer IV as is true for neocortex. Differentiation of primate cingulate gyrus (PCG) is discussed in detail in Chapter 3. In the context of a progressive differentiation, sampling cingulate cortex for diagnostic assessment is more difficult than it may initially appear. Evaluation of a 'limbic' preference (or category) requires sampling sACC, while designation of a 'neocortical' preference requires sampling in dPCC. The aMCC straddles these cortical trends in the cingulate gyrus.

Table 32.1 provides αSN counts for layers V/VI of three levels of the cingulate gyrus in the same total area of measurement. Case #4 was not included because it had a very high level of tau-immunoreactive, neuropil threads, as discussed below, and was at a late stage of AD. In contrast, the first three cases either did not have neurofibrillary markers of AD (#1) or were at an early stage in the medial temporal lobe with no or minor evidence of neuritic pathology in the cingulate gyrus (cases #2 and #3). Although there were variations among the three cases and case #1 had the highest overall densities of αSN-immunoreactive neurons, they were least dense in sACC and aMCC and highest in dPCC. Indeed, there were about 60% more αSN in dPCC than in either of the other regions and this is the subregion in which we begin this analysis.

α-Synuclein Associations with Neurodegeneration in dPCC

Expression of LB in the substantia nigra is associated with neuron losses and this is expected for the cingulate gyrus. However, the thin H&E sections and diffuse nature of LBs mitigate against a clear demonstration of this linkage. Here we use thicker sections, an α-synuclein antibody, and a NeuN-immunoreacted control case to guide assessment of neuron densities in each layer.

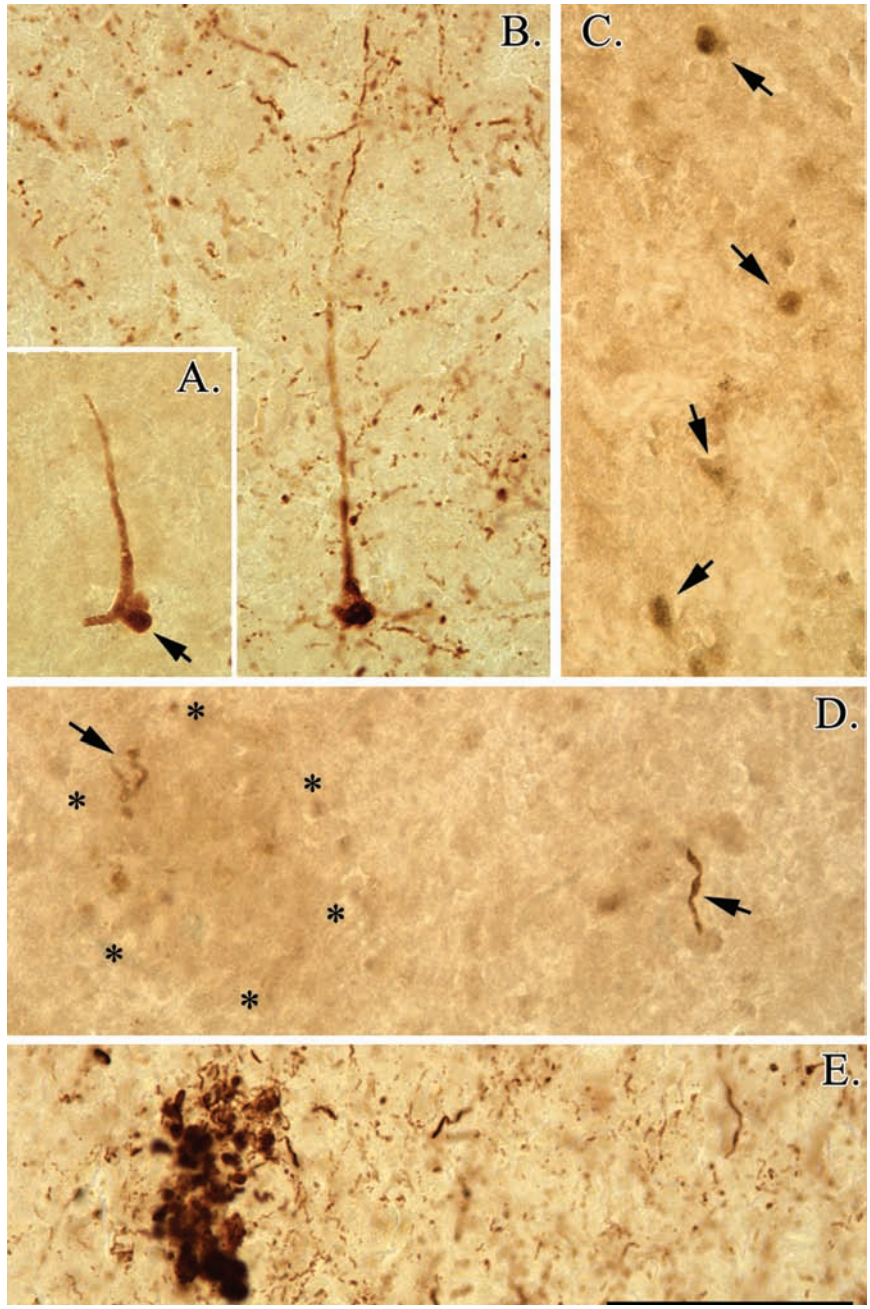

Fig. 32.2 Examples of LB and αSN in two cases; #3, A–C and #1, D–E. A. α-synuclein-immunoreactive neuron with arrow pointing to a LB and B. AT8-ir neuron in an adjacent section. C. Most α-synuclein-ir neurons have a moderate to dense and granular reaction in the perikaryon; some are marked here with arrows and the pia is to the right of this picture. D. α-synuclein-ir neurites are found in cingulate cortex as marked here with arrows from area 25. The arrow on the left identifies an ir-neurite that may be located in a neuritic plaque as suggested by the round structure in layer V of area 25 as outlined with asterisks. E. Shows a typical AT8-positive neuritic plaque in the same area and layer as in D for size comparisons. Scale, 100 μm.

Layer V: Match

Given that the highest numbers of αSN are in the dPCC, this seems to be the ideal site to assess neuron densities in layers V and VI. In fact, most of the αSN in the cingulate gyrus in these four cases were in layer V and this focuses the question of linkage. Figure 32.3 shows layer Va in area 23a in a number of preparations. The high level of αSN is evident as is the high neuron loss in this layer. The NeuN section provides a context to emphasize that many neurons have been lost in this layer, although some large neurons remain. Also, there is almost no amyloid-β42 (Aβ42) in this same layer as discussed in detail below. Thus, although some αSN may be lost over time, their preference for deep layers and associated neuron losses suggests a link between the marker and neuron losses.

Layer III: Mismatch?

Although occasional αSN are in layer III in dPCC, the general fact is that throughout the cingulate gyrus most

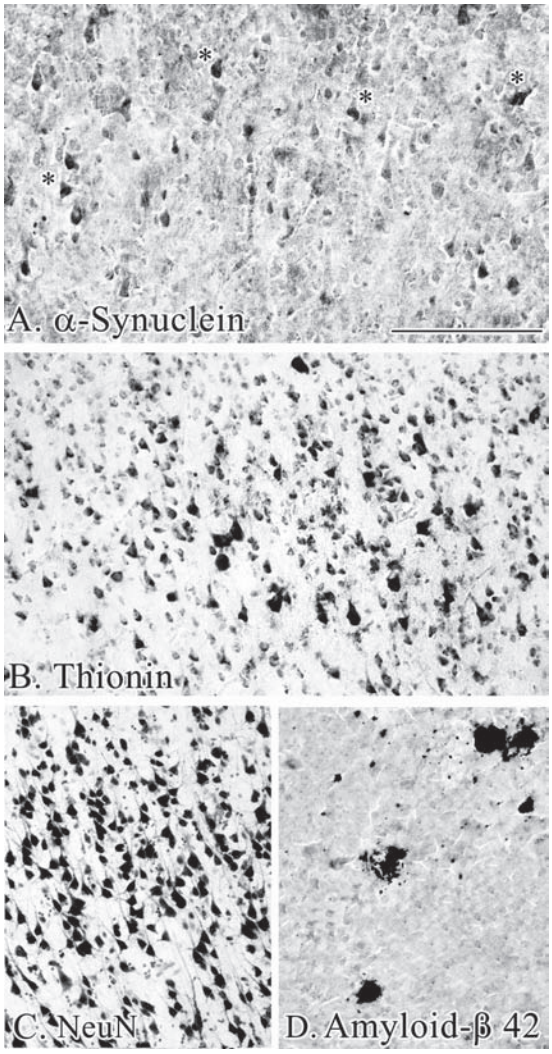

Fig. 32.3 αSN in area d23a of case #1 (4 are marked with asterisks in A). B. Shows significant neuron losses in layer Va compared with the control NeuN reacted tissue (C.). There was almost no Aβ42 in this layer (D.) and very little was in more superficial layers. Calibration bar, 200 μm.

of these neurons are in layer V and fewer in layer VI. Consider neuron densities in layer III of each major division of the cingulate gyrus in the following figures. Layer III of area d23b has substantial neuron losses (Fig. 32.4). In area 25 the losses are clear but spotty in layer III (Fig. 32.7). Finally, in areas of the aMCC region there is substantial neuron degeneration in layer III. Another example of layer III αSN is shown below for a sample in pMCC; but there are still just a limited number. It is possible, of course, that αSN in external layers were removed by phagocytosis in an earlier stage in these cases. Alternatively, most damage to layer III neurons, as well as layer II where it occurs, may not be associated with the deposition of α-synuclein and other mechanisms of neurodegeneration need to be considered.

α-Synuclein/Amyloid-β42 Interrelations

Harding and Halliday (2001) could not differentiate between DLB and PDD based on the densities of cortical LBs including those in area 24 and the only outstanding DLB features were parahippocampal LBs and plaque densities. Although it is well established that PDD and AD are often comorbid (Perl *et al*., 1998), the issue here is whether or not a classical AD marker is coexpressed with αSN in DLB. Pletnikova *et al*. (2005) reported enhanced cortical α-synuclein deposits in brains with high loads of Aβ peptides, and Mann *et al*. (1998) showed greater deposition of Aβ42(43) than Aβ40 in DLB than in sporadic AD, although they were unable to find a correlation with LBs in DLB. Thus, both markers co-exist in the same brains, there may be an interaction between their neurotoxic properties, and this provides an explicit hypothesis to guide a laminar analysis of cingulate cortex.

The Aβ42-immunoreative diffuse plaques are much more heavily expressed in DLB than is Aβ40 (Mann *et al*., 1998). In this latter study the ratio of Aβ40:Aβ42/43 in DLB was 6.6±5.1 versus AD 47.8±39.7, while the percent load in DLB for Aβ42 was 5.2±2.3 and Aβ40 0.36±0.39. In contrast, AD had an Aβ42 percent load of 7.4±2.1 and Aβ40 of 3.7±3.5. Importantly, neurofibrillary tangles (NFT) in parahippocampal cortex reflected Braak stage III/IV, while neocortex expressed relatively few NFT. There appeared to be no link between the expression of NFT in these separate regions. The Consensus Guidelines refer to AD pathology in DLB and neocortical NFT are rare and diffuse and neuritic plaques are usually present. The CERAD description of the LB variant of AD (Heyman *et al*., 1999) also emphasized that neocortical NFT are infrequent in DLB compared with AD without co-expression of LB.

To evaluate linkages between Aβ42, neurodegeneration and associated αSN deposition mainly in layer V, area d23b is used in Figure 32.4 as a representative of dPCC. Arrows point to aggregates of neurons in the otherwise severely damaged tissue. Indeed, the loss of neurons in #4 is so great that the oval surrounds the only truly intact layer IIIc. Although some neurons are in layers V and VI, there is severe neuron loss in these layers in all cases. Co-registration of the thionin and Aβ42 sections provides an ideal test of the extent to which layer V αSN, neurodegeneration, and diffuse plaque load are linked. The answer is yes and no. Case #4 has the heaviest load of Aβ42 and greatest overall neuron loss; however, this is patent AD in the cingulate gyrus. In the DLB cases, layer V has a moderate plaque

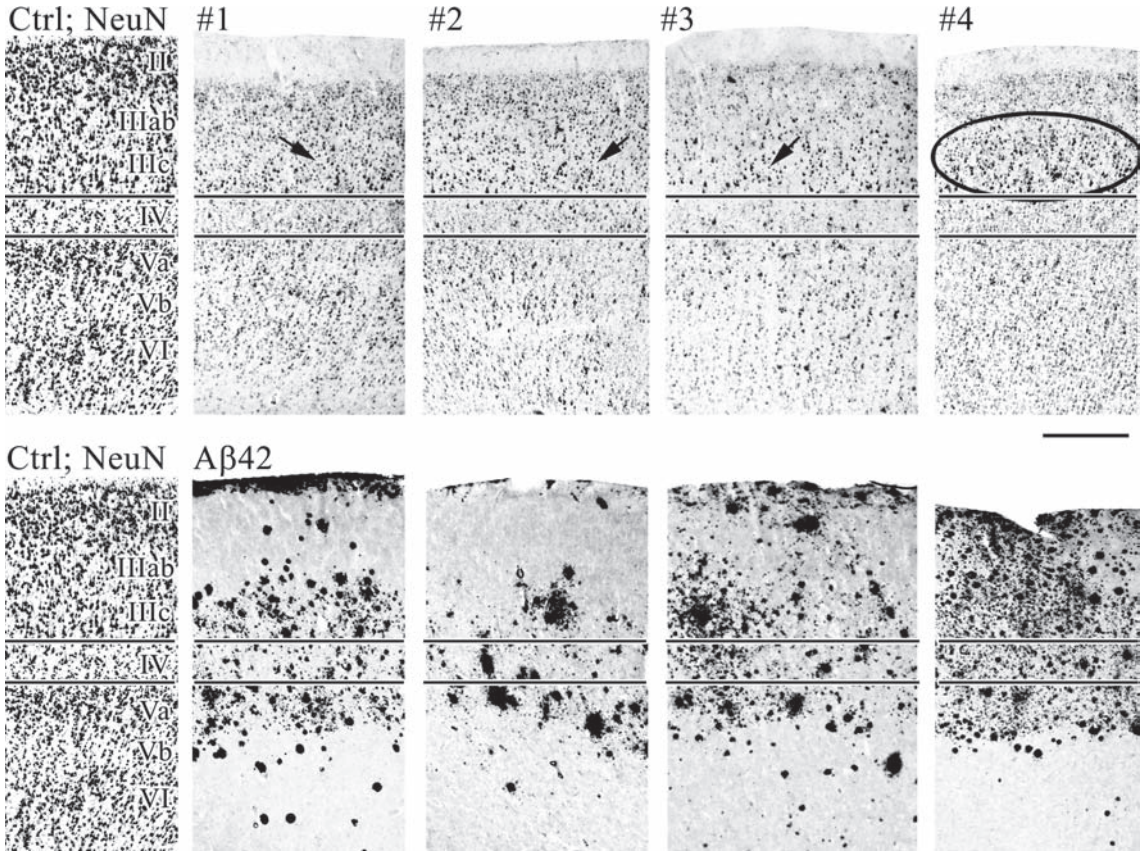

Fig. 32.4 Neurons and Aβ42 in area d23b. Layer IV borders are shown and the Ctrl; NeuN is a standard to assess adjacent thionin-stained sections. Arrows point to aggregates of neurons in the otherwise severely damaged tissue. Indeed, the loss of neurons in #4 is so great that the oval surrounds the only 'intact' layer IIIc. Severe neuron loss is in most layers in all cases. Case #4 has the heaviest Aβ42 load and overall neuron loss. The DLB cases have a moderate plaque load and severe neurodegeneration in layers IIIc, IV, and Va; however, layers IIIab and VI have a low plaque burden yet neuron densities are severely compromised. Calibration bar, 500 μm.

load and severe neurodegeneration/αSN. However, layers IIIab, IV, and VI have a very low plaque burden yet neuron densities are severely compromised.

Thus, there is a linkage between Aβ42-immunoreactive diffuse plaque load and neuron losses/αSN, however, the linkage is not tight because many other layers also have neuron loss but express little or no Aβ42. Of course, there are many possible explanations including the neurotoxic actions of soluble Aβ42 that is not detected with immunohistochemistry and the anatomical observations leave open the issue of whether all αSN-mediated cingulate neurodegeneration is associated with Aβ42.

Neurofibrillary Deposits Appear Irrelevant to Early α-Synuclein Deposition

The question of the extent of AD neuropathology in the four DLB cases is raised because there was a generally low level or complete lack of NFT in the cingulate gyrus and throughout the neocortex in general. Although neurofibrillary degeneration occurs in AD with LB, NFT are rare in these cases compared with AD alone (Gearing *et al.*, 1999; Heyman *et al.*, 1999). This was true for the present cases in which only rare NFT occurred throughout the cingulate gyrus even in the case that had the diagnosis of probable AD. The Braak stages are provided in Table 32.1 and the expression of neuropil threads (AT8-immunoreactive neurites) are shown for area 25 in Figure 32.5. The relative density and distribution is the same throughout the cingulate gyrus for all DLB cases. The figure shows that only case #4 had a high level of neuropil threads. The other three cases had much less and case #2 had a few neuritic plaques scattered throughout the cortex. Thus, it appears that neurodegeneration must be linked to the expression of α-synuclein and possibly Aβ42 but not neurofibrillary degeneration.

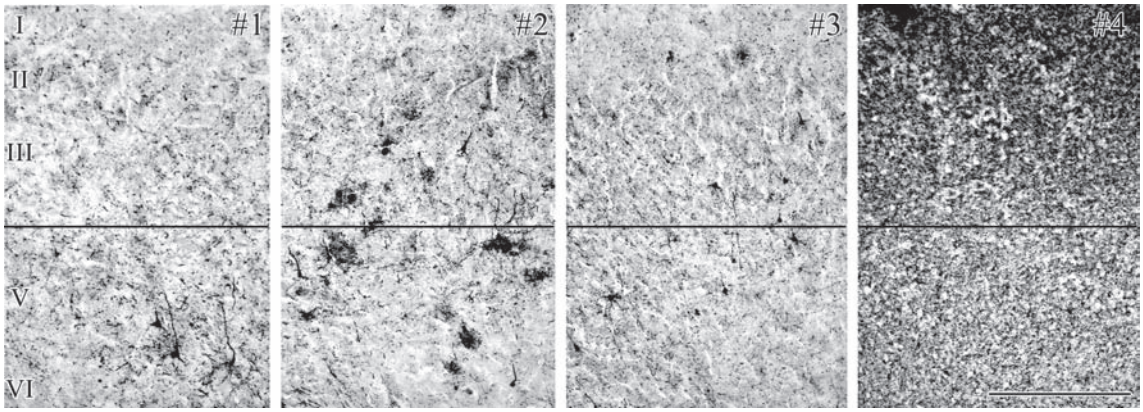

Fig. 32.5 Neurofibrillary degeneration in area 25 shown with the AT8 antibody. The sections are aligned at the layer III/V border (horizontal line). The first three cases show mostly sparse neurites and a few neurons with neurofibrillary tangles (NFT); case #2 had a number of neuritic plaques and case #4 had extensive neurites though there were only rare NFT buried in this rich plexus. Scale bar, 500 μm.

Limbic Pathology in Subgenual ACC

As noted above, the cingulate gyrus undergoes a progressive differentiation which begins in subgenual and pericallosal cortices and extends caudally and dorsally into dPCC. To the extent that a case can be classified as 'limbic' in DLB, it must have evidence for profound involvement of sACC areas 25, s24, and s32. Thionin stains of area 25 clearly demonstrate neuron losses in this area, but they are variable. As shown in Figure 32.6, most neurons in case #1 are missing in inner layer III and inner V, while layers II, top of III, V, and VI are less impacted though still show some signs of neuron loss. In case #2, layers III, and VI are profoundly impacted, in case #3 layers III and VI are mainly impacted and all but layer II has severe neurodegeneration in case #4. Thus, the case with Braak stage V AD had the greatest overall neuron losses and this might not be attributed to DLB. In the three DLB cases (#1-3), layer II and outer layer III are the least impacted. This confirms the Braak staging of LBs in PD which shows these latter layers to be impacted late in disease progression.

It is striking that layers with the lowest Aβ42 load have the least neuron losses in area 25 in DLB cases: #1, layers Vb and VI; #2, layer II, top of III and VI; #3, layers III and VI. This lack of association is most apparent in cases #2 and #3 where Aβ42 load is low or negligible in layer II and the top of layer III. Finally, Aβ42 expression is highest in layer Va where neuron losses appear to be minimal. Thus, low-to-moderate levels Aβ42 do not appear to be closely associated with neurodegeneration in sACC.

Anterior Midcingulate Damage and the Rostral Cingulate Premotor Area

As LB diseases involve movement disorders, the midcingulate region has two somatotopically distinct skeletomotor control systems (Chapters 1 and 5), and the Consensus Guidelines (McKieth *et al.*, 1996) recommend sampling in its anterior division (aMCC), it must be considered the extent to which this region is impacted in DLB. As layer Vb neurons in sulcal aMCC project to the spinal cord, it is possible that some aspect of intentional movement impairment results from damage to this region. Although the cingulate motor areas are in the cingulate sulcus, we begin this analysis with the gyral surface area a24a′/b′ as these areas are also part of most postmortem diagnostic procedures.

Area a24b

Layer Va appears to be virtually intact in the first three cases shown in Figure 32.7 (emphasized by solid line at layer Va/Vb border). While layer Va is least affected of all layers in case #4, the degeneration throughout this case is severe. Case #1 has the most preserved neuron densities, although layer VI is missing (asterisk). Cases #2 and #3 have substantial neurodegeneration in layer III in addition to having lost layer VI and layer II is damaged in case #2. Two key questions emerge from these cases. First, as layer Vb in areas a24c′, p24c′, and 24d contains neurons that project to the spinal cord, is it intact in area a24b′? Looking below the layer Va/Vb border in cases #1–#3 suggests that, although some neurons are

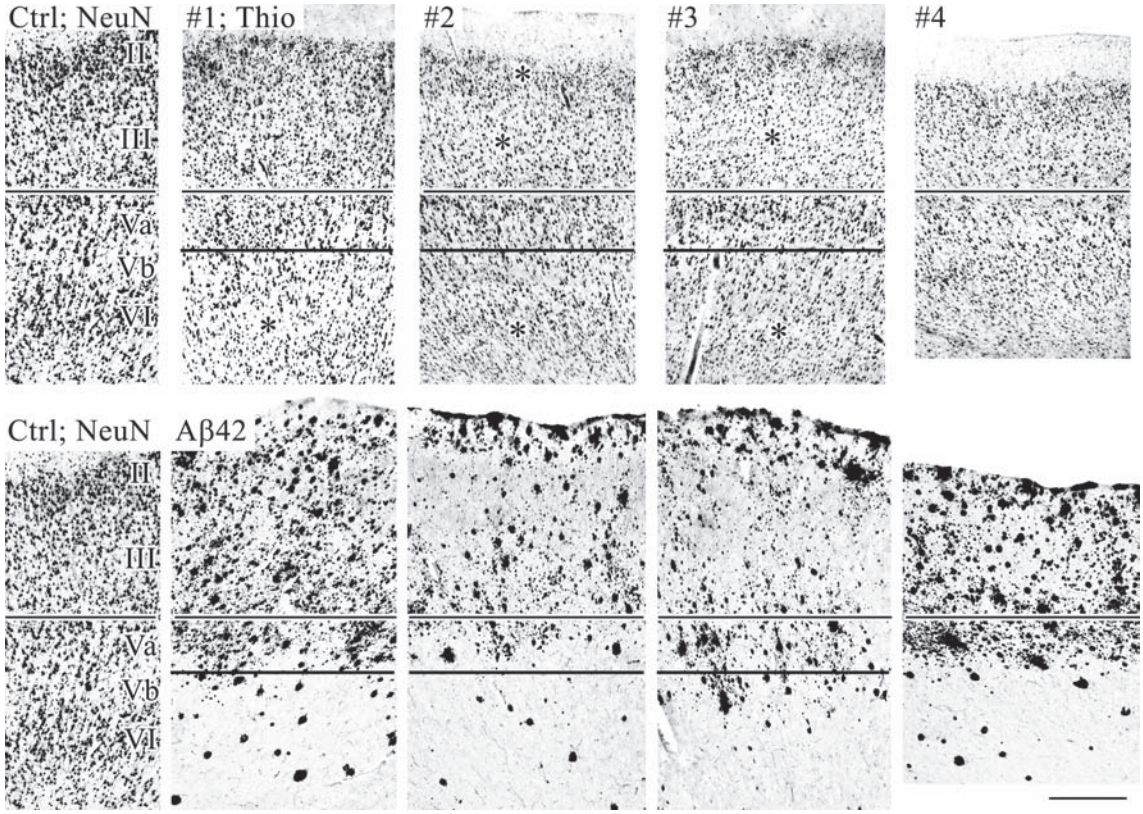

Fig. 32.6 Neuron densities in area 25 (top row) and Aβ42 expression matched in adjacent sections and co-registered to the above sections (bottom row; except for repeat of the "Ctrl; NeuN" The control (Ctrl; NeuN) provides a standard for comparison to with the thionon sections. Places of pronounced neuron losses and marked with asterisks; although other sites are impacted such as the large neurons in layer III of #1. Although layer II tends to have normal densities of nuerons, expect #2, layers III, V and VI are profoundly involved. Case #1 has greatest neuron loss in layer VI where there is virtually no Aβ42, while the reverse is true for all other layers. In contrast, Cases #2 and #3 have moderate Aβ42 in layer III where there is neuron loss and layer Va appears normal, although it contains significant Aβ42 in both cases.

in this layer (i.e., it is not lost like layer VI), most large neurons seem to have been lost. In the next paragraph there is a consideration of the cingulate motor cortex. Second, is there a link between the deposition of Aβ42 and neuron losses? Case #1 argues against that conclusion because it has heavy Aβ42 in superficial layers where least neuron loss occurs, while it has no Aβ42 in layer VI where greatest losses occurred. The same could be said about case #4; however, there is extensive neuropil thread deposition in this case even in the deep layers suggesting other mechanisms of neurodegeneration. In cases #2 and #3, there are diffuse Aβ42 plaques in layer III where there is substantial neuron losses, however, layer Va appears to be close to intact as in case #3, the highest level of plaque formation is in this layer. Once again, layer VI is almost completely destroyed yet there are only a few dense core plaques in this layer. It appears that there is only a tenuous link between Aβ42 deposition and neurodegeneration in aMCC.

Area a24c′

Neuron losses in area a24b′ might predict that adjacent cortex in the cingulate sulcus would also have losses. As neurons in layer Vb of area a24c′ project to the spinal cord, layers V and VI were magnified for Figure 32.8 from this area to evaluate such a possibility. In addition, NeuN and thionin sections are shown for the control case to provide a guide as to how these two methods differ in showing the architecture of a cingulate layers V and VI in area a24c′ in the control and cases #1–#3. The NeuN and thionin (NeuN, Thio) are shown for the control case so that comparison with the thionin case sections can be better appreciated. The extent of neurodegeneration appears to build in these three cases; places of particularly high neuron losses are marked with asterisks. The degeneration appeared to be greatest in the following layers: case #1, layer V; case #2, layers Vb and VI; and case #3, each layer.

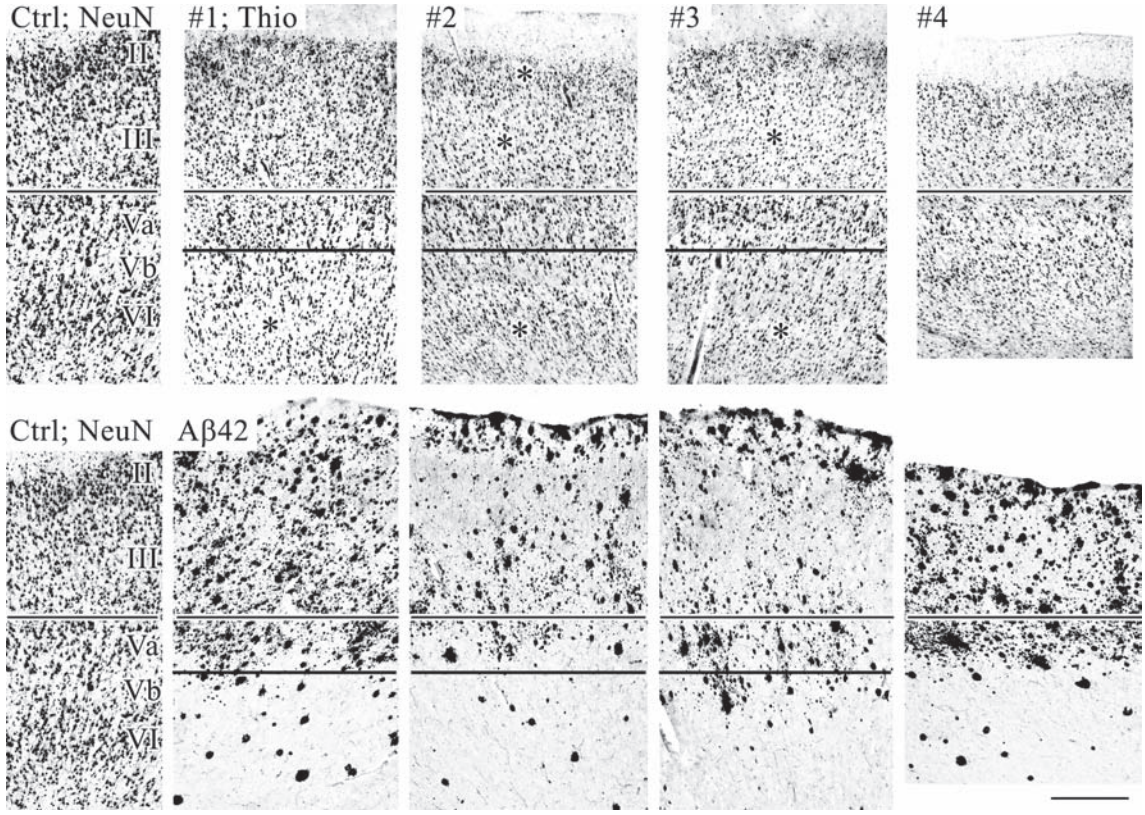

Fig. 32.7 Area a24b' from aMCC in thionin and Aβ42 preparations. Layer Va is virtually intact in the first three cases (solid line at layer Va/Vb border for emphasis). While layer Va is least affected of all layers in case #4, the neuron loss is severe. Case #1 has the most preserved neuron densities, although layer VI is missing (asterisk). Cases #2 and #3 have substantial neuron losses in layer III, most of layer VI is lost and layer II is damaged in case #2. Layer Vb in cases #1–#3 shows that, although some neurons are in this layer (i.e., it is not lost like layer VI), most large neurons have been lost. The distribution of Aβ42 is heavy in superficial layers where least neuron loss occurs, while there is no Aβ42 in layer VI where greatest losses occurred. In cases #2 and #3, there are diffused Aβ42 plaques in layer III where there is substantial neuron losses, however, layer Va appears to be close to intact and in case #3, the highest level of plaque formation is in this layer. Layer VI is almost completely destroyed yet there are only a few dense core plaques in this layer. Calibration bar, 500 μm.

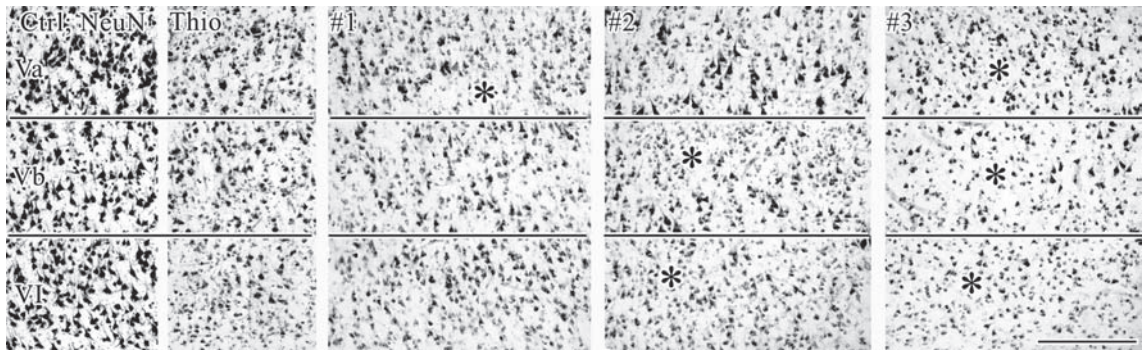

Fig. 32.8 Layers V and VI in area a24c' in the control and cases #1–#3. The NeuN and thionin (NeuN, Thio) are shown for the control case so that comparison with the thionin case sections can be better appreciated. The extent of neurodegeneration appears to build in these three cases; places of particularly high neuron losses are marked with asterisks. The degeneration appeared to be greatest in the following layers: case #1, layer V; case #2, layers Vb and VI; and case #3, each layer. Calibration, 200 μm.

Dopamine hypothesis and rostral cingulate premotor damage

The DA hypothesis of PDD and DLB is well supported by an extensive literature on the deposition of LB in the substantia nigra, the role of this damage in early motor symptoms, and its clear association with nigral neurodegeneration. As dementia in PD appears after the motor signs in PD and cortical pathology is more extensive at this point, it is likely that dementia results from changes in the cerebral cortex. It has never been made clear that the DA dysfunction hypothesis applies to aMCC; not just the substantia nigra and its projections into the striatum. This oversight likely is the result of technical considerations. From a technical point of view, most *in vivo* imaging emphasizes the basal ganglia where DA transporters and receptors are most dense and generally undetected in the cerebral cortex (e.g., Colloby *et al.*, 2004). Partial volume averaging greatly hinders detecting more diffuse signals throughout the cerebral cortex even in the cingulate gyrus where DA innervation is the highest as discussed in Chapter 7.

The rCPMA receives the most dense innervation of DAergic fibers as shown with tyrosine hydroxylase immunohistochemistry (Vogt *et al.*, 1997). The contribution of the dorsal aMCC (i.e., areas a24c′, and 32′) are involved in a number of executive functions including mismatch detection and selection among response alternatives as discussed in detail in Chapter 12. This subregion also has a role in reward (Chapters 7 and 8) and premotor responses to noxious stimulation (Chapter 14) are also well documented. The rCPMA has extensive connections to the spinal cord in those instances where such motor regulation is required (Chapters 1 and 5), although decision making, information processing in this subregion does not require a skeletomotor output. Thus, one of the important themes of this volume is the role of aMCC in cognitive functions with a specific emphasis on reward, nocifensive behaviors, and response selection.

DLB and PDD have two specific impacts on information processing in the aMCC/rCMA. First, it produces a DA deafferentation lesion that likely impairs reward coding and response selection among rewarded and nonrewarded behaviors. Second, phosphorylation and/or nitration of α-SN evokes death of neurons in layer V including those that project to the spinal cord. This latter event may contribute to a loss of cognitive guiding of complex movement. Thus, although the LB dementias have profound extrapyramidal motor signs including rigidity, resting tremor, and bradykinesia, they also have cortical damage that leads to a loss of motor control at the most complex decision making level of processing. Cingulate-mediated impairments have not been demonstrated and there are no neuropsychological tests to probe this damage and follow its progression.

Posterior Midcingulate Damage and the Caudal Cingulate Premotor Area

The caudal cingulate premotor area (cCPMA) is comprised a number of different cytoarchitectural areas including areas p24c′, 24d, and 23c (Vogt *et al.*, 2005). These areas interface with the dPCC and provide mechanisms for coupling visuospatial orientation with motor outputs (Vogt *et al.*, 2006; Chapter 13) and disruption of this interface leads to various visuoconstructional deficits as discussed in Chapter 34. As highest levels of αSN and neuron losses are in the PCG (Table 32.1), it is possible there is a high level of neuron loss in the sulcal cortex of the posterior MCC where the cCMA is located. Indeed, both αSN and neuron losses are much greater in this region than in aMCC.

Figure 32.9 shows cortex on the dorsal bank of the midcingulate gyrus at the level 6 sampling site (Fig. 32.1B). In the face of severe neurodegeneration, it is not possible to make subtle cytoarchitectural differentiations and we refer to this cortex as areas p24c′/24d. Although scattered neurons are in all layers, there are severe losses and shrinkage of those remaining. Layer Vb contains the largest neurons in area 24d as shown in the control case and these neurons make spinal projections as discussed in Chapters 1 and 5. Clearly, these neurons are either greatly shrunken or not present in case #1. Although there are many αSN-positive neurons in layer Vb (asterisks in Fig. 32.9), αSN neurons are present throughout the cortex including layer III as also marked with asterisks in this figure. Co-registrations of Aβ42 showed a moderate level of diffuse plaques in the deep layers much like that shown in Figure 32.7 for area a24b′. In other words, the linkage between neuron losses and Aβ42 is weak but present in layer V.

Site of First Damage and Staging Lewy Body Diseases

Fundamental to staging a neurodegenerative disease is a precise hypothesis about where the first cortical damage appears and the mechanism by which it spreads or evolves. Efforts to stage both DLB and PDD have been made and the primary nidus of damage and its subsequent progression determines the evolution of clinical symptoms, the timing and content of neuropsychological testing necessary to diagnose the dementia, and the value of particular treatment interventions. Our hypothesis is that the primary nidus of cingulate damage in DLB is in pMCC and dPCC. Amazingly, this is the same nidus identified in a frontal variant case of mild cognitive impairment (Johnson *et al.*, 2003; Chapter 33). What does the literature state or imply about the site of first cingulate damage and why do we conclude that it is in pMCC/dPCC? This issue is ideally addressed in the

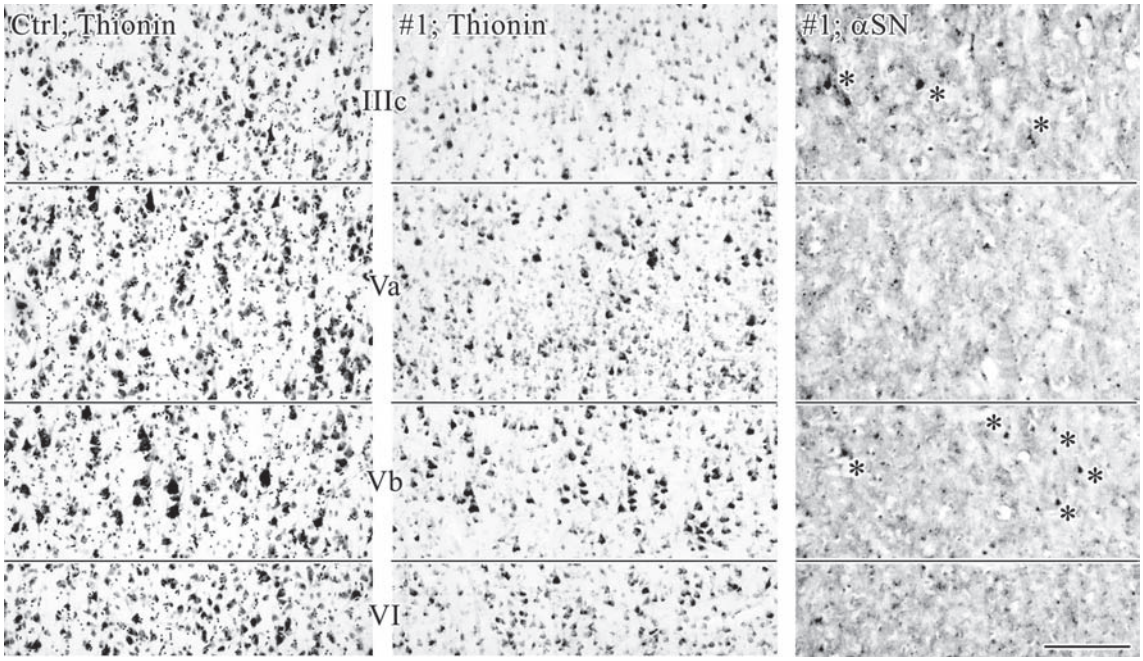

Fig. 32.9 Cortex on the dorsal bank of the midcingulate gyrus in areas p24c'/24d. A thionin section was photographed from the control for comparison of neuron densities with in the same subregion in case #1. The largest neurons in layer Vb that likely project to the spinal cord can be seen in the control (Ctrl) and are either greatly shrunken or missing in case #1. Severe neurodegeneration is in all layers (#1); not just layer Vb. The αSN are mainly in layer Vb but also layer IIIc (asterisks for emphasis). Calibration bar, 200 μm.

cingulate gyrus because of its cytoarchitectural diversity and systematic structural differentiation beginning in the callosal sulcus.

It is of interest to this problem that distinguishing between DLB and PDD is controversial and the primary sites of cortical damage could be the same in both diseases. Richard *et al*. (2002) performed a pilot clinicopathological assessment of ten cases and concluded that two groups could only be distinguished in terms of the time course of clinical symptoms; not by any qualitatively unique differences in symptoms or postmortem pathology. As sections were used from the entire cingulate gyrus, no regional inferences can be drawn about the progression of DLB or PDD in this region. Mauri *et al*. (2002) evaluated the progression and stages of LB deposition in DLB and observed earliest LBs in layers V–VI, then in layer III, and finally layer II with progression beginning in the amygdala and proceeding to limbic cortex and neocortex. Hishikawa *et al*. (2003) classified cases of DLB according to the three categories suggested by the Consensus Guidelines and showed silver-stained LBs that were rare in the cingulate gyrus in the brainstem-predominant category, more in cingulate, parahippocampal, and insular cortices in the limbic category and many throughout limbic cortex and neocortex in the neocortical category. They also made the pivotal observation that the densities and distribution of α-synuclein, coiled inclusions in glia were the same; a linkage that was maintained in aMCC. This suggests a more global vulnerability in cingulate cortex.

In many ways these dynamics are similar to those reported by Braak *et al*. (2003) for PDD. They reported presymptomatic stages 1 and 2 with mainly medulla oblongata and olfactory bulb LBs, in stages 3 and 4 there is involvement of the substantia nigra with minor changes in the cortex, and finally symptomatic stages 5 and 6 with severe cortical involvement. In terms of the cingulate gyrus, it appears that sACC and pACC, and pericallosal areas are first sites of insult in PDD and progression from there engages ever more dorsal and caudal cingulate cortex.

The stages reported in most studies are indeed linked but the question in the cingulate gyrus remains where the first site of damage is located. Limbic and neocortical LB are highly correlated and this suggests a simple progression from one to the other (Gómez-Tortosa *et al*., 1999). Indeed, the buildup of LBs in aMCC seems to be progressive (Hishikawa *et al*., 2003). Thus, studies based on a single slice including the cingulate gyrus suggest this subregion is first involved in the 'limbic' stage and progression involves a greater number of αSN in the one site sampled in the neocortical stage. The limitation of sampling only one level of the cingulate gyrus is that it cannot address progressive changes along the

entire gyrus. The present analysis of seven levels of the cingulate gyrus suggests the first site of damage in DLB is in pMCC/dPCC. In contrast, the Braak stages emphasize initial pathology in sACC and progression follows the cytoarchitectural differentiation trend from rostral and ventral to caudal and dorsal cingulate cortex for PDD. It is possible that there is a different origination site in DLB and PDD and this will influence progressive changes.

The pMCC/dPCC nidus: Primary site of cingulate damage in DLB

The present cases suggest that pMCC and dPCC are the site of first damage in the cingulate gyrus. This is based on the following considerations. It is assumed that the most severe damage occurs in that area/subregion that is first impacted. A corollary of this is that any disease marker that is uniformly expressed provides no information about the site of disease onset or its progression. In terms of total αSN, it appears that the pMCC/dPCC have the greatest density of these intracellular inclusions in DLB, while ACC has significantly fewer. Moreover, the most severe neuron losses were encountered in pMCC and dPCC and not in sACC or aMCC. This seems to conflict with the Braak staging of PDD which suggests disease initiation in sACC. Surprisingly, of the three DLB cases here, case #1 has a pure DLB and more diffuse Aβ42 plaque deposits in area 25 (Fig. 32.6) than in any other area. It may be that co-deposition of these two markers in DLB and variances with PDD produce two different pathology initiation sites and two different patterns of cingulate disease progression.

Mechanisms of Neurodegeneration in the Cingulate Gyrus

Consideration of the topography and laminar patterns of α-synuclein and amyloid-β deposition and their association with neuron losses in the cingulate gyrus are consistent with three mechanisms of cell death. These mechanisms are well explored in the literature and are briefly reviewed here to provide a context and source for future studies of cingulate neurodegenerative mechanisms. Some of these may eventually be resolved to a point where we will understand why the cingulate gyrus is selectively vulnerable early in DLB and PDD to such pathological insults and they certainly may be interrelated as suggested at the end of this section.

α-Synuclein phosphorylation, folding, and aggregation

Alpha-synuclein is a normal constituent of presynaptic axon terminals and is a member of a novel class of targets for G protein-coupled receptor kinases (Pronin *et al*., 2000). It has been shown that the distribution of α-synuclein in the synaptic terminal is regulated by neuronal activity (Fortin *et al*., 2005); however, its specific synaptic function is unknown. Although α-synuclein is used to identify neurons that may degenerate in DLB and PDD, it has been argued that early expression of this protein may be a neuroprotective event that becomes lethal later in a disease process (Harrower *et al*., 2005; Chandra *et al*., 2005).

One mechanism of inactivating α-synuclein and potentially turning it into an insoluble and neurotoxic agent is phosphorylation of serine 129. In *Drosophila* replacing this single amino acid with alanine suppresses DAergic neuron loss produced by expression of human α-synuclein. Moreover, phosphorylation at Ser129 enhances α-synuclein toxicity (Chen & Feany, 2005). Transfection of α-synuclein into human and rodent cell lines showed that it is constitutively phosphorylated predominantly on Ser129 and less efficiently on Ser87 (Okochi *et al*., 2000). In addition to regulating the function of α-synuclein via phosphorylation/dephosphorylation pathways, it appears that these processes can lead to neuron death and are relevant to mechanisms in the cingulate gyrus.

Mutations of the αSN gene generate DLB (Zarranz *et al*., 2004), have been associated with inheritance of early-onset PD (Polymeropoulos *et al*., 1997) and there is a dose-effect associated with earlier and more severe PD (Ibanez *et al*., 2004). An interesting study of αSN protein and message levels in human neurons suggested that the soluble protein persists at normal levels despite reductions in mRNA suggesting a defect in protein clearance (Cantuti-Castelvetri *et al*., 2005).

Amyloid-β42 deposition

Deposition of Aβ42 in diffuse plaques is known to occur early in cognitive impairments associated with dementia (Parvathy *et al*., 2001). Although Aβ42 deposits are linked with αSN in cingulate layer V, the general load in 'non-AD' cases is moderate to low. That is to say, Aβ42 does not reach the level seen in AD and need account for only a small proportion of overall neurodegeneration. Moreover, layers II, III, and VI tend to not express Aβ42 and this mechanism of neuron death may not be invoked, although soluble forms of the peptide could be at work that cannot be detected with immunohistochemistry. Nevertheless, a link between these markers is a common finding in DLB (McKeith *et al*., 1996; Mann *et al*., 1998; Pletnikova *et al*., 2005). Moreover, amyloid peptides appear to interact with native α-synuclein to form insoluble fibrils which contribute to LB deposition (Yagi *et al*., 2005) and this interaction could contribute to amyloid fibril formation and neurodegeneration in the cingulate gyrus.

Oxidative Stress and Peptide Nitration

The presence of 3-nitro-tyrosine, a peroxynitrite modified form of tyrosine, in PD suggests the presence of oxidative injury in LB containing neurons (Good *et al.*, 1998). Indeed, nitrated α-synuclein is present in cortical neurons in DLB (Giasson *et al.*, 2000) suggesting that oxidative stress may be prominent. Furthermore, nitration of α-synuclein initiates the formation of aggregates and could initiate DLB (Paxinou *et al.*, 2001) and an increase in highly perodizable lipids have been detected in the amygdala and frontal cortex of incidental LB disease (Dalfo *et al.*, 2005). Although α-synuclein may be directly nitrated to generate neurotoxic aggregates, oxidative damage need not act only via this mechanism and could induce neuron death through other mechanisms in layers that do not express αSN or Aβ peptides. As αSN are deposited in layers II and III late in DLB (Marui *et al.*, 2002), and they were not detected in these layers in the present study, it is assumed that neurodegeneration in these layers occurs by additional or alternative mechanisms.

Neurodegenerative Mechanism Interactions

Links between DLB and AD mechanisms of neurodegeneration may occur via interactions among amyloidogenic peptides in the cingulate cortex. It appears that ser129 phosphorylation of α-synuclein may be an early step in DLB. Further phosphorylations, though less efficient, could lead to insoluble forms of the peptide and blocking normal clearance mechanisms. A secondary interaction of phospho-α-synuclein with other amyloid peptides such a amyloid-β peptides could enhance deposition of α-synuclein and insoluble fibrils that lead to patent neurodegeneration in DAergic neurons throughout the brain as well as cortically vulnerable neurons including those in layer V of the cingulate gyrus. The reasons for early vulnerability of layer V neurons likely hold the clue to rational design of therapeutics to halt DLB progression.

A Cingulate Role for Dementia in Parkinson's Disease

Cognitive impairment in PDD is critically dependent on disruption of cingulate cortex. A highly significant correlation exists in PDD between the Clinical Dementia Rating score (a surrogate marker of dementia) in PDD and area 24 αSN (Kövari *et al.*, 2003). This latter study concluded that LB pathology limited to entorhinal and ACC/MCC may be sufficient to predict cognitive decline in PD. Parenthetically, NFT had no such predictive value. Mattila *et al.* (2000) also reported that the number of LB in the cingulate gyrus significantly correlated with cognitive impairment in PD; although the number of NFT in the temporal lobe was also significant in this series and the evaluation was a retrospective hospital file assessment based on the Global Deterioration Scale. Although the neuropsychological deficit is not specified and the location of cingulate neuropathology not well specified, it is important that a linkage exists and with the regional model of the cingulate gyrus along with well-localized neuropathological assessment in DLB, it may be possible to characterize a number of highly specific hypotheses about the linkage between DLB/PDD and cingulate impairments.

Cingulate-Mediated Symptoms in Lewy Body Diseases: Ideomotor and Constructional Impairments Following Impaired Visuospatial-Motor Coupling

Different parts of the cingulate gyrus have been implicated in LB diseases. Albin *et al.* (1996) used imaging of DLB and implicated aMCC and PCC, the aMCC samples in neuropathological studies emphasize varying levels of involvement of this region as discussed above in terms of the rCMA, and the present study shows that while the entire cingulate gyrus can be involved in DLB, the pMM/dPCC nidus is likely the first site of α-synuclein-mediated damage and greatest neuron losses. It is now possible to use the four-region neurobiological model presented in Chapter 1 to assess cingulate-mediated symptoms in DLB.

A thorough evaluation of neuropsychological deficits in patients with DLB was provided by Salmon *et al.* (1996). This group was compared with an 'equally impaired group of pure' AD. Their conclusion is most important, 'One of the most striking aspects of the performance of the DLBD patients was the severity of their impairment on tests of visuospatial and visuocontructive ability.' As visuospatial and visuocontructional processing are among the primary functions of pMCC and dPCC, it is possible that some of the primary neuropsychological deficits in DLB can be explained by damage in this region of the cingulate gyrus.

Cingulate Hypotheses Derived from Alzheimer's Disease

The coexpression of LBs in AD (LB variant; Heyman *et al.*, 1999) is just one reason for considering the functional impairment of cingulate cortex in AD as a prelude to that in DLB. Another reason is that a subgroup of AD with visuospatial deficits (Martin, 1990) likely experience first damage in dPCC and it is well known that region is glucose hypometabolic in the amnestic subgroup of mild cognitive impairment that evolves into AD (Minoshima *et al.*, 1997; Chapters 33 and 34). A CERAD comparison of AD with and without

Lewy bodies identified only one major neuropsychological difference between these groups of patients; those with LBs had delayed recall from a learned word list with more than twice having a deficiency in the LB group (Heyman *et al*., 1999). Just as interesting is the fact that both groups had similar visuospatial function and constructional praxis and there were no differences in cognitive fluctuations, visual hallucinations, delusions, recurrent falls, and parkinsonism (Gómez-Tortosa *et al*., 1999).

Constructional apraxias are well known in AD and are evaluated by drawing pentagons. A drawing disturbance without general impairment of intelligence, visual, or motor capabilities results from parietal lobe lesions (Zadikoff & Lang, 2005), although the specific role of PCC is not well appreciated. In view of the fact that Cormack *et al*. (2004) observed a high degree of constructional apraxia in DLB, it is an important observation that NFT in dPCC are significantly correlated with constructional apraxia in AD (Giannakopoulos *et al*., 1998). This latter group also observed a correlation between NFT in dPCC and spatial disorientation in AD (Giannakopoulas *et al*., 2000). Finally, spatial disorientation is correlated with glucose hypometabolism in PCC in AD (Hirono *et al*., 1998). Thus, there is a tight link between dPCC damage in AD and alterations in visuospatial and visuoconstructive abilities.

Visuospatial and Visuoconstructive Deficits Following pMCC/dPCC Damage: A Common Theme

Evidence for the general contribution of the DLB nidal region is not limited to findings in AD. Indeed, strokes in this region also produce spatial disorientation (reviewed in Chapter 13) and possibly impaired executive functions that depend on visuospatial coordination as reported in some cases of mild cognitive impairment (Chapter 33). Thus, damage to dPCC is associated with spatial disorientation and constructional apraxia regardless of the source of damage and this includes the deposition of α-synuclein in dPCC neurons and their subsequent death in DLB.

Circuitry studies of dPCC suggest a coordinated substrate in which functional disorganization between pMCC and dPCC can lead to constructional apraxias. A rich body of experimental monkey studies and basal glucose metabolism correlations in human show there are heavy interconnections between dPCC and the sulcal cingulate cortex that contains the cCPMA (reviewed in Chapters 5 and 13). One of the primary functions of dPCC is orientation of the head, limbs, and body in space and the dense projections of this subregion into the cCPMA provides a mechanism for guiding complex movements such as those required for drawing figures and moving to goals in visual space. Moreover, it has recently been suggested that this region is involved intentions and one's consequent actions (den Ouden *et al*., 2005) further supporting the role of this region in complex, premotor planning. Thus, damage to dPCC and often pMCC in stroke, AD, DLB, and PDD, leads to deafferentation of the cCPMA and in some diseases overt neuronal damage thereto. Highly selective, neuropsychological tests are needed that will herald the earliest neuronal damage to this subregion and its underlying circuits. Eventually, the pMCC and dPCC may become one of the primary sites of diagnostic and therapeutic interventions in neurodegenerative diseases.

References

Albin, R. L., Minoshima, S., D'Amato, C. J., Frey, K. A., Kuhl, D. A., & Sima, A. A. (1996) Fluro-deoxyglucose positron emission tomography in diffuse Lewy body disease. *Neurology 47*: 462–466.

Ballard, C. G., Aarsland, D., McKeith, I., O'Brien, J., Gray, A., Cormack, F., Burn, D., Cassidy, T., Starfeldt, R., Larsen, J-P., Brown,R., & Tovee, M. (2002) Fluctuations in attention. PD dementia vs DLB with parkinsonism. *Neurology 59*: 1714–1720.

Braak, H., Del Tredici, K., Rüb, U., de Vos, R. A.I., Jansen, E. N.H., & Braak, E. (2003) Staging of brain pathology related to sporadic Parkinson's disease. *Neurobiol Aging 24*: 197–211.

Braak, H., Rüb, U., Steur, J., Tredici, K. D., & de Vos, R. A.I. (2005) Cognitive status correlated with neuropathological stage in Parkinson disease. *Neurology 64*: 1404–1410.

Burton, E. J., Karas, G., Paling, S. M., Barber, R., Williams, E. D., Ballard, C. G., McKieth, I. G., Scheltens P., Barkhof, F., & O'Brien, J. T. (2002) Patterns of cerebral atrophy in dementia with Lewy bodies using voxel-based morphometry. *NeuroImage 17*: 618–630.

Cantuti-Castelvetri, I., Klucken, J., Ingelsson, M., Ramasamy, K., McLean, P., Frosch, M. P., Hyman, B. T., & Standaert, D. G. (2005)Alpha-synulein and chaperones in dementia with Lewy bodies. *J Neuropathol Exper Neurol 64*: 1058–1066.

Chandra, S., Fornai, F., Kwon, H-B., Yazdani, U., Atasoy, D., Liu, X., Hammer, R. E., Battaglia, G., German, D. C., Castillo, P. E., & Sudhof, T. C. (2004) Double-knockout mice for α- and β-synucleins: Effect on synaptic functions. *Proc Natl Acad Sci USA 101*: 14966–14971.

Chandra, S., Gallardo, G., Ferandez-Chacon, R., Schluter, O. M., & Sudhof, T. C. (2005) α-Synuclein

cooperates with CSPα in preventing neurodegeneration. *Cell 123*: 383–396.

Chen, L., & Feany, M. B. (2005)α-Synuclein phosphorylation controls neurotoxicity and inclusion formation in a *Drosophila* model of Parkinson disease. *Nat Neurosci 8*: 657–663.

Colloby, S. J., O'Brien, J. T., Fenwick, J. D., Firbank, M. J., Burn, D. J., McKeith, I. G., & Williams, E. D. (2004) The application of statistical parametric mapping to ^{123}I-FP-CIT SPECT in dementia with Lewy bodies, Alzheimer's disease and Parkinson 's disease. *NeuroImage 23*: 956–966.

Cormack, F., Aarsland, D., Ballard, C., & Tovee, M. J. (2004) Pentagon drawing and neuropsychological performance in dementia with Lewy bodies, Alzheimer's disease, Parkinson's disease and Parkinson's disease with dementia. *Int J Geriatr Psychiatry 19*: 371–377.

Dalfo, E., Portero-Otin, M., Ayala, V., Martinez, A., Pamplona, R., & Ferrer, I. (2005) Evidence of oxidative stress in the neocortex in incidental Lewy body disease. *J Neuropathol Exper Neurol 64*: 816–830.

Den Ouden, H. E.M., Frith, U., Frith, C., & Blakemore, S-J. (2005) Thinking about intentions. *NeuroImage 28*: 787–796.

Dickson, D. W. (2001) Alpha-synuclein and the Lewy body disorders. *Curr Opin Neurol 14*: 423–432.

Ditter, S. M., & Mirra, S. S. (1987) Neuropathologic and clinical features of Parkinson's disease in Alzheimer's disease patients. *Neurology 37*: 754–760.

Firbank, M. J., Colloby, S. J., Burn, D. J., McKeith, I. G., & O'Brien, J. T. (2003) Regional cerebral blood flow in Parkinson's disease with and without dementia. *NeuroImage 20*: 1309–1319.

Fortin, D. L., Nemani, V. M., Voglmaier, S. M., Anthony, M. D., Ryan, T. A., & Edwards, R. H. (2005) Neural activity controls the synaptic accumulation of α-synuclein. *J Neurosci 23*: 10913–10921.

Gearing, M., Lynn, M., & Mirra, S. S. (1999) Neurofibrillary pathology in Alzheimer disease with Lewy bodies. *Arch Neurol 56*: 203–208.

Giannakopoulos, P., Duc, M., Gold, G., Hof, P. R., Michel. J-P., & Bouras, C. (1998) Pathologic correlates of apraxia in Alzheimer disease. *Arch Neurol 55*: 689–695.

Giannakopoulos, P., Gold, G., Duc, M., Michel, J-P., Hof, P. R., & Bouras, C. (2000) Neural substrates of spatial and temporal disorientation in Alzheimer's disease. *Acta Neuropathol 100*: 189–195.

Giasson, B. I., Duda, J. E., Murray, I. V. J., Chen, Q., Souza, J. M., Hurtig, H. I., Ischiropoulos, H., Trojanowski, J. Q., & Lee, V. M-J. (2000) Oxidative damage linked to neurodegeneration by selective α-synuclein nitration in synucleinopathy lesions. *Science 290*: 985–989.

Goedert, M., Jakes, R., & Vanmechelen, E. (1995) Monoclonal antibody AT8 recognizes tau protein phosphorylated at both serine 202 and threonine 205. *Neurosci Lett 189*: 167–169.

Gómez-Tortosa, Newell, K., Irizarry, M. C., Albert, M., Growden, J. H., & Hyman, B. T. (1999) Clinical and quantitative pathologic correlates of dementia with Lewy bodies. *Neurology 53*: 1284–1291.

Good, P. F., Hsu, A., Werner, P., Perl, D. P., & Olanow, C. W. (1998) Protein nitration in Parkinson's disease. *J Neuropathol Exper Neurol 57*: 338.

Guo, L., Itaya, M., Takanashi, M., Mizuno, Y., & Mori, H. (2005) Relationship between Parkinson disease with dementia and dementia with Lewy bodies. *Parkinsonism Related Disord 11*: 305–309.

Harding, A. J., & Halliday, G. M. (2001) Cortical Lewy body pathology in the diagnosis of dementia. *Acta Neuropathol 102*: 355–363.

Harrower, T. P., Michell, A. W., & Barker, R. A. (2005) Lewy bodies in Parkinson's disease: Protectors or perpetuators? *Exper Neurol 195*: 1–6.

Heyman, A., Fillenbaum, G. G., Gearing, M., Mirra, S. S., Welsh-Bohmer, K. A., Peterson, B., & Pieper, C. (1999) Comparison of Lewy body variant of Alzheimer's disease with pure Alzheimer's disease. *Neurology 52*: 1839–1844.

Hirono, N., Mori, E., Ishii, K., Ikejiri, Y., Imamura, T., Shimomura, T., Hashimoto, M., Yamashita, H., & Sasaki, M. (1998) Hypofunction in the posterior cingulate gyrus correlates with disorientation for time and place in Alzheimer's disease. *J Neurol Neurosurg Psychiatry 64*: 552–554.

Hurtig, H. I., Trojanowski, M. D., Galvin, J., Ewbank, D., Schmidt, M. L., Lee, V. M-Y., Clark, C. M., Glosser, G., Stern, M. B., Gollomp, S. M., & Arnold, S. E. (2000) Alpha-synuclein cortical Lewy bodies correlate with dementia in Parkinson's disease. *Neurology 54*: 1916–1921.

Kövari, E., Gold, G., Herrmann, F. R., Canuto, A., Hof, P. R., Bouras, C., & Giannakopoulos, P. (2003) Lewy body densities in the entorhinal and anterior cingulate cortex predict cognitive deficits in Parkinson's disease. *Acta Neuropathol 106*: 83–88.

Ibanez, P., Bonnet, A. M., Debarges, B., Lohmann, E., Tison, F., Pollak, P., Agid, Y., Durr, A., & Brice, A. (2004) Causal relation between alpha-synuclein gene duplication and familial Parkinson's disease. *Lancet 364*: 1169–1171.

Ishii, K., Imamura, T., Sasaki, M., Yamaji, S., Sakamoto, S., Kitagaki, H., Hashimoto, M., Hirono, N., Shimomura, T., & Mori, E. (1998). Regional cerebral glucose metabolism in dementia with Lewy bodies and Alzheimer's disease. *Neurology 51*: 125–130.

Mann, D. A.M., Brown, S. M.P., Owen, F., Baba, M., & Iwatsubo, T. (1998) Amyloid β protein (Aβ) deposition in dementia with Lewy bodies: predominance of $A\beta_{42(43)}$ and paucity of $A\beta_{40}$ compared with sporadic Alzheimer's disease. *Neuropathol Appl Neurobiol 24*: 187–194.

Martin, A. (1990) Neuropsychology of Alzheimer's disease: The case for subgroups. In M. F Schwartz (Ed.) *Modular Deficits in Alzheimer-type Dementia* (pp. 145–175), Cambridge, MA: MIT Press.

Mattila, P. M., Rinne, J. O., Helenius, H., Dickson, D. W., & Roytta, M. (2000) Alpha-synuclein-immunoreactive cortical Lewy bodies are associated with cognitive impairment in Parkinson's disease. *Acta Neuropathol 100*: 285–290.

Mauri, W., Iseki, F., Nakai, T., Miura, S., Kato, M., Ueda, K., Kosaka, K. (2002) Progression and staging of Lewy pathology in brains from patients with dementia with Lewy bodies. *J Neurolog Sci 195*: 153–159.

McKeith, I. G., Galasko, D., & Kosaka, K., *et al*. (1996) Consensus guidelines for the clinical and pathologic diagnosis of dementia with Lewy bodies (DLB): Report of the consortium on DLB international workshop. *Neurology 47*: 1113–1124.

Minoshima, S., Giordani, B., Berent, S., Frey, K. A., Foster, N. L., & Kuhl, D. E. (1997) Metabolic reduction in the posterior cingulate cortex in very early Alzheimer's disease. *Ann Neurol 42*: 85–94.

Okochi, M., Walter, J., Koyama, A., Nakajo, S., Baba, M., Iwatsubo, T., Meijer, L., Kahle, P. J., & Haass, C. (2000) Constitutive phosphorylation of the Parkinson's disease associated α-synuclein. *J Biolog Chem 275*: 390–397.

Parvathy, S., Davies, P., Haroutunian, V., Purohit, D. P., Davis, K. L., Mohs, R. C., Park, H., Moran, T. M., Chan, J. Y., & Buxbaum, J. D. (2001) Correlation between Aβx-40-, Aβx-42-, and Aβx-43-containing amyloid plaques and cognitive decline. *Arch Neurol 58*: 2025–2032.

Paxinou, E., Chen, Q., Weisse, M., Giasson, B. I., Norris, E. H., Rueter, S. M., Trojanowski, J. Q., Lee, VM-Y., & Ischiropoulos, H. (2001) Induction of α-synuclein aggregation by intracellular nitrative insult. *J Neurosci 21*: 8053–8061.

Perl, D. P., Olanow,W., & Calne, D. (1998) Alzheimer's disease and Parkinson's disease: Distinct entities or extremes of a spectrum of neurodegeneration? *Ann Neurol 44* (Suppl 1): S19–S31.

Pletnikova, O., West, N., Lee, M. K., Rudow, G. L., Skolasky, R. L., Dawson, T. M., Marsh, L., & Troncoso, J. C. (2005) Aβ deposition is associated with enhanced cortical α-synuclein lesions in Lewy body diseases. *Neurobiol Aging 26*: 1183–1192.

Polymeropoulos, M. H., Lavedan, C., Leroy, E. *et al*. (1997) Mutation in the α-synuclein gene identified in families with Parkinson's disease. *Science 276*: 2045–2047.

Pronin, A. N., Morris, A. J., Suruchov, A., & Benovic, J. L. (2000) Synucleins are a novel class of substrates for G protein-coupled receptor kinases. *J Biol Chem 275*: 26515–26522.

Richard, I. H., Papka, M., Rubio, A., & Kurlan, R. (2002) Parkinson's disease and dementia with Lewy bodies: One disease or two? *Mov Disord 17*: 1161–1165.

Saito, Y., Kawashima, A., Ruberu, N. N., Fujiwara, H., Koyama, S., Sawabe, M., Arai, T., Nagura, H., Yamanouchi, H., Hasegawa, M., Iwatsubo, T., & Murayama, S. (2003) Accumulation of phosphorylated α-synuclein in aging human brain. *J Neuropathol Exper Neurol 62*: 644–654.

Sakamoto, M., Uchihara, T., Hayashi, M., Nakamura, A., Kikuchi, E., Mizutani, T., Mizusawa, H., & Hirai, S. (2002) Heterogeneity of nigral and cortical Lewy bodies differentiated by amplified triple-labeling for alpha-synuclein, ubiquitin, and thiazin red. *Exper Neurol 177*: 88–94.

Salmon, D. P., Galasko, D., Hansen, L. A., Masliah, E., Butters, N., Thal, L. J., & Katzman, R. (1996) Neuropsychological deficits associated with diffuse Lewy body disease. *Brain Cog 31*: 148–165.

Talairach, J., & Tournoux, P. (1988) *Co-planar Stereotaxic Atlas of the Human Brain*. Stuttgart: Georg Thieme Verlag.

Vogt, B. A., Martin, A., Vrana, K. E., Absher, J. R., Vogt, L. J., & Hof, P. R. (2000) Multifocal cortical neurodegeneration in Alzheimer's disease. In A. Peters, & J. H. Morrison (Eds), *Cerebral Cortex* (pp. 553–601), *14*, "Neurodegenerative and Age-related Changes in Structure and Function of Cerebral Cortex".

Vogt, B. A., Vogt, L., Farber, N. B., & Bush, G. (2005) Architecture and neurocytology of the monkey cingulate gyrus. *J Comp Neurol 485*: 218–239.

Vogt, B. A., Vogt, L., & Laureys, S. (2006) Cytology and functionally correlated circuits of human posterior cingulate areas. *NeuroImage 29*: 452–466.

Vogt, B. A., Vogt, L. J., Nimchinsky, E. A., & Hof, P. R. (1997) Primate cingulate cortex chemoarchitecture and its disruption in Alzheimer's disease. In F. E. Bloom, A. Björkund, & T. Hökfelt (Eds), *Handbook of Chemical Neuroanatomy* (pp. 455–528).

Vogt, B. A., Vogt, L. J., Perl, D. P., & Hof, P. R. (2001) Cytology of human caudomedial cingulate,

retrosplenial, and caudal parahippocampal cortices. *J Comp Neurol 438*: 353–376.

Yagi, H., Kusaka, E., Hongo, K., Mizobata, T., & Kawata, Y. (2005) Amyloid fibril formation of α-synuclein is accelerated by preformed amyloid seeds of other proteins. *J Biol Chem 280*: 38609–38616.

Zadikoff, C., & Lang, A. E. (2005) Apraxia in movement disorders. *Brain 128*: 1480–1497.

Zarranz, J. J., Alegre, J., Gomez-Esteban, J. C., *et al.* (2004) The new mutation, E46K, of α-synuclein causes Parkinson and Lewy body dementia. *Ann Neurol 55*: 164–173.